Heterogeneity of the Glass Fiber Surface from Inverse Gas Chromatography

T. I. Bakaeva, C. G. Pantano, C. E. Loope, and V. A. Bakaev*

Department of Material Science and Engineering and Department of Chemistry, 152 Davey Laboratory, Penn State University, University Park, Pennsylvania 16802

Received: April 7, 2000

The chromatographic peak profiles of hexane and butanol on a column packed with E-glass fibers show that the surface of the fiber is homogeneous for hexane and heterogeneous for butanol. The distributions of adsorption sites in energy and entropy are obtained separately by a new method. This method is a generalization to heterogeneous surfaces of the widely used method of determination of the entropy and the energy of adsorption from the temperature dependence of the Henry constant. It is shown that the assumption that the entropy of adsorption can be taken as constant for all the adsorption sites (such an assumption is usually made in the literature) is not true for butanol. Another new result is the plot of entropy vs energy for different sites. This plot allows one to exclude the unreliable portion of the energy distribution

1. Introduction

The surface atomic structure of silicate glasses is the basis for understanding their surface properties on an atomic level. However, the experimental methods for exploring the surface atomic structure of glasses are limited. In our recent papers, we set forth a new method for exploring the surface atomic structure using a physically adsorbed molecule as a probe of the surface atomic structure.[1,2] Specifically, one creates a model glass surface by computer simulation, then simulates adsorption on that model surface and compares simulated adsorption characteristics with real ones to validate the model of the glass surface. In the course of this work, it has already been shown that the continuous random network that is the basis for all the silicate glass atomic structures extends up to the surface of amorphous silica without coordination defects such as nonbridging oxygen, double rings, etc.[1,3] It has also been demonstrated that the shape of an isotherm of adsorption is quite sensitive to the atomic structure of a model silica surface.[2]

The isotherms of adsorption that were simulated and compared with experimental data in these studies were for Ar and CO_2. They were measured by a conventional volumetric technique on relatively high surface area (ca. 2 m^2/g) glass fibers (glass wool).[2,4] It was shown that the standard method used in ref 4 cannot be employed with glass fibers of considerably lower specific surfaces like, e.g., one used in this paper (0.2 m^2/g; 7 μm diameter). Since the majority of industrial glass fibers have specific surfaces on the same order of magnitude or less than that used in this paper (diameters equal or larger than 7 μm), here we describe another method of measuring their adsorption characteristics: inverse gas chromatography (IGC).

There have already been several applications of IGC to the study of glass surfaces.[5−10] They were carried out on glass fibers (glass wool) with specific surfaces of about 0.2−0.3 m^2/g,[5−8] on glass beads with specific surface of 1.2 m^2/g,[10] and on the surfaces of glass capillaries 50−500 μm i.d.[9] In addition, there are many papers dedicated to the application of IGC to the study of the surfaces of high surface area silica, alumina, and other high surface area oxides. These results were reviewed recently in refs 11−16.

The first application of IGC to glass fibers was concerned with the measurement of isotherms of adsorption of *n*-alkanes and some polar molecules up to the saturation vapor pressure.[5] They used a detector of relatively low sensitivity (katharometer). From these data, the spreading pressure was calculated that made it possible to evaluate contributions to the solid/liquid surface energy. All other IGC studies of low surface area glasses were carried out at (supposedly) infinite dilution (zero coverage).

The isotherm of adsorption is a function of concentration (partial pressure) of a solute. At infinite dilution of a solute (in IGC a gas phase is a mixture of an inert carrier gas and an active solute) an isotherm can be approximated by a straight line. The slope of the line is the Henry constant. The region of concentration where the isotherm can be approximated by a straight line is called the Henry region. In this region and under assumption that the kinetics of adsorption is sufficiently fast (which is usually true for an open surface like that of glass fiber), the elution chromatographic peak is usually a symmetric Gaussian curve. The position of its maximum, which does not depend on the injected amount of solute, is the retention time that determines the Henry constant.

The advantage of IGC is that it can use a very sensitive chromatographic detector like the flame ionization detector (FID) that allows one to work in a region of very low solute concentrations, which in many cases is the Henry region. Thus, the measurement of the Henry constants is a very popular direction of adsorption IGC. In particular, the review papers[12,14−16] are totally devoted to this application of IGC. The result of such an IGC experiment is usually presented as a pair of thermodynamic functions for the solute/surface interaction: the Henry constant (that depends on temperature) and the approximately temperature independent enthalpy. When these thermodynamic functions are measured for different solutes on the same surface, they can be separated into components that characterize the surface in its interaction with various substances of industrial interest (e.g., organic adsorbates). This separation is based on empirical relationships reviewed in ref 12. Subsequently, it is possible to study how those surface characteristics change due to various modifications of the surface.

In a manner similar to the study of high surface area oxides,[14−16] IGC studies on low surface area glasses essentially followed the same route[6−8,10] (ref 9 is mainly qualitative). However, these studies failed to obtain symmetric peak profiles

10.1021/jp0013457 CCC: $19.00
Published on Web 08/16/2000

for all the solutes. This means that they did not reach the linear Henry region in some cases. In these cases they adopted a procedure essentially similar to that described in ref 7. In ref 7, they worked in the region of relatively high solute concentrations (because a katharometer was used as a detector) and obtained asymmetric peak profiles even for *n*-alkanes. But in the previous paper[6] where FID was used, they showed that the peak profiles of *n*-alkanes become symmetric in the region of very small solute concentration; in other words, they were able to reach the Henry region for *n*-alkanes with FID. Thus, they proposed to determine the Henry constants from asymmetric peak profiles on the basis of the largest retention time corresponding to the minimal detectable concentration of the solute. They emphasized that this is an unreliable method that can be used only for comparative studies when, for example, one compares the characteristics of surfaces subjected to different modifications.

Essentially the same method was used in other studies of low surface area glasses when they obtained asymmetric peak profiles for alcohols and other polar adsorbates.[8,10] In fact, they implied that the Henry region of solute concentration can always be reached with such a sensitive detector as FID and in the temperature range of usual commercial chromatographs used in their studies.

The fact that this might be not true follows from the studies of adsorption of nitrogen and rare gases on the surfaces of glasses, some other oxides, and metals (see a review in ref 17, pp 42−51). It has been shown that even in ultrahigh vacuum (down to 10^{-11} mmHg) isotherms of adsorption on a glass surface were not linear at the boiling temperatures of the adsorbates.

The reason for that is the heterogeneous nature of the glass surface.[18] This means that adsorption activity of this surface is concentrated in special sites called adsorption sites (or just sites) and these sites are different in their adsorption activity measured, e.g., by the energy of interaction of a site with an adsorbed molecule. (Below, we call the energy, entropy, and free energy of a molecule interacting with a site just the energy, etc. of the site.) Such a heterogeneous surface is usually characterized by the energy distribution of sites.[17] In our previous computer simulation of a vitreous silica surface and adsorption of water on this model surface, we discovered these sites as local minima of the water molecule−silica surface interaction.[1] These are places where the intensity of the surface electrostatic field is especially strong. This field is irregular at the amorphous silica surface, which is the reason for the surface heterogeneity with respect to water adsorption. On the same reasoning, one may expect heterogeneity of the amorphous silica surface with respect to all the molecules that interact strongly with the surface electrostatic field. These are polar molecules such as alcohols or quadrupolar molecules such as CO_2. In our next paper[2] we have shown that our model silica surface is really heterogeneous with respect to adsorption of CO_2. However, it turned out to be almost homogeneous with respect to adsorption of Ar.[2] (In the Langmuir model that is, in fact, considered here, a homogeneous surface is a special case of a heterogeneous surface when all the sites are identical.[17]) This is because the interaction of an Ar molecule with the irregular surface electrostatic field is much weaker than that of polar molecules. One may expect the same behavior for other nonpolar molecules such as *n*-alkanes. Furthermore, there is ample reason to believe that the situation will be similar also on the surfaces of E-glass fibers used in this work.

This means that it may happen that the Henry constant is not an appropriate characteristic of a fiber glass surface. First, the ultrahigh vacuum experiments mentioned above suggest that the Henry region can be unreachable in IGC with such polar solutes as, e.g., alcohols at their boiling temperatures because the sensitivity of FID is many orders of magnitude lower than that of ultrahigh vacuum manometers. This will be discussed in more detail in the last paragraph of section 4. Second, even if one manages to reach the Henry region for a heterogeneous surface (e.g., by raising the temperature way above the boiling point of adsorptive), one would obtain the Henry constant averaged over all the adsorption sites.[11] This is only an average characteristic of the surface adsorption activity. We will show below that from IGC one can obtain a more detailed characteristic of glass fiber surface: the free energy (energy) distribution of adsorption sites. Such a characteristic is equivalent to ascribing the separate Henry constant to each adsorption site.

The calculation of the site energy distribution from adsorption IGC data is certainly not new. It is reviewed in refs 11, 13, 17, and 19. What is new here is that we obtain not only the energy but also the entropy distribution and the entropy/energy relationship for sites. The latter can be used to test the validity of the energy distribution. Only some part of the energy distribution obtained in this work passed this test. We believe that this is connected to the fact that the column packed with low surface area glass fiber has very low efficiency. The Ideal model of chromatography that is the basis for IGC does not work very well for such columns. This is discussed in more detail in subsection 3.1.

2. Experimental Section

We used a HP5890 series II (Hewlett-Packard) gas chromatograph. The stainless steel column was 2 m long with 5.3 mm inner diameter. Its inner surface was Silcosteel-treated (Restek Corporation) to make it inert. It was packed with 27 g of water-sized E-glass fiber (PPG). The BET specific surface of the fiber measured by Kr was 0.22 m^2/g. The diameters of threads measured by the electron microscope were about 7 μm.

In our experiments the pressure drop on the column varied from 0.3 to 0.6 psi so that the pressure gradient correction factor j deviated from unity by less than 2% and the flow rate of the carrier gas (helium) varied from 30 to 90 mL/min. The lower flow rate was achieved by placing at the output of the column a narrow capillary that increased the pressure drop over the column. No difference between final results was observed with or without that capillary.

The FID detector used in this work was calibrated with the help of a standard capillary column (Rtx-5, Restek Corp.). The constant of calibration was determined as

$$C_{\mathrm{FID}} = Qn_{\mathrm{C}}/S \tag{1}$$

where Q is the quantity of a solute (hexane or butanol) injected into the column, S is the peak area, and n_{C} is the effective carbon number of the solute. In this calibration we used acetone/butanol and methylene chloride/hexane mixtures and obtained: $C_{\mathrm{FID}} = (1.45 \pm 0.01) \times 10^{-5}$ nmol/(counts·s); $n_{\mathrm{C}} = 6$ for hexane; $n_{\mathrm{C}} = 3.4$ for butanol. To convert the peak profile $y(t)$, where y is measured in *counts* (internal units of HP5890) and t is time, into $C(t)$, where C is the concentration of solute, we used the following relationship

$$C(t) = C_{\mathrm{FID}}y(t)/(n_{\mathrm{C}}v_{\mathrm{o}}) \tag{2}$$

where v_{o} is the volume flow rate of the carrier gas (C is negligibly small with respect to the concentration of the carrier gas) at the output of the column. The scale was linear in the

whole range of concentration used, and the calibration constant was also checked for our column.

A chromatographic experiment usually consisted of two parts: First, the elution curve was obtained at the fixed column temperature. After that the temperature of the column automatically increased at the rate of 40 °C/min up to 250 °C and stayed fixed at that level for 30 min. Experimental points were recorded with the frequency of 5 Hz. Thus, the total volume of information corresponding to, e.g., Figures 2 and 3 consists of 24 000 experimental points. The background signal in our case was on the order of 10 counts so that even the smallest signals in Figures 2 and 3 were about three orders of magnitude higher than the background (random errors). This is a huge amount of information in comparison to that usually obtained by direct adsorption measurements (as, for example, in our previous paper[4]). These data were transferred to a separate PC and processed by a special FORTRAN code.

Adsorbates were *n*-heptane and butanol. They were used without purification as obtained from Aldrich. Methane was used as a nonsorbed solute. It was obtained from Restek Corp. (as the methane cylinder kit).

3. Models

3.1. Ideal Model of Chromatography. The processing of experimental data in this paper is based on the Ideal model of chromatography described by the following mass balance equation[20]

$$\frac{\partial C}{\partial t} + F\frac{\partial q}{\partial t} + u_0\frac{\partial C}{\partial z} = 0 \tag{3}$$

where C and q are the concentrations of the component in the mobile and stationary phases, respectively, z is column length, t is time, $F = (1 - \epsilon)/\epsilon$ with ϵ porosity of the column packing, and u_0 is the mobile phase velocity. Finally, it is assumed in the Ideal model that adsorption kinetics is so fast (on the time scale of a chromatographic experiment) that q and C are connected by an equilibrium adsorption equation and

$$\frac{\partial q}{\partial t} = \frac{\partial q}{\partial C}\frac{\partial C}{\partial t} \tag{4}$$

The profile of a chromatographic peak is $C_l(t) = C(t;z=l)$ where l is the length of the column. It is a solution to eqs 3 and 4 (with appropriate initial and boundary conditions). It is seen from eqs 3 and 4 that $C_l(t)$ depends on the isotherm of adsorption $q(C)$ and the parameters of the column F, l, and u_0.

The Ideal model eq 3 has an analytic solution. This solution, which is the basis of the elution of the characteristic point (ECP) method of IGC, is[21]

$$V_N(C) = j v_0(t_R(C) - t_M) = \frac{dN}{dC} \tag{5}$$

Here V_N is the net retention volume,[21] $t_R(C)$ is the retention time of a characteristic point corresponding to the concentration C, t_M is the retention time of nonsorbed solute, and v_0 is the volumetric flow rate at the column outlet. j in eq 5 is the pressure gradient correction factor. This correction factor is not contained in eq 3 that does not take into account the compressibility of the mobile phase. This is one of the assumptions of the model mentioned above. In our case, this assumption is well justified because the pressure drop over our column was always less than 0.3 psi and j was very close to unity (see Table 2.1 in ref 21). Finally, N in eq 5 is the total number of occupied sites (total adsorption) on all the surface in the column corresponding to equilibrium concentration C in the gas phase.

One can integrate a dN/dC plot to obtain the isotherm of adsorption. The isotherm is usually reduced to the unit of mass of the absorbent or to the unit area of its surface. Below, we designate adsorption by the unit area of surface by a or use coverage θ, which is the ratio of a to its value at the monolayer coverage. The isotherm of adsorption, in turn, makes it possible to determine some characteristics more directly by describing the state of a surface: the Henry constant (subsection 3.2) or distribution of adsorption sites in energy (DASE) (subsection 3.3).

It has been shown that the Ideal model gives accurate results only for columns of very high efficiency.[22] This is definitely not the case for glass fibers because they have very low specific surfaces. The Ideal model cannot be used with columns of low efficiency to determine DASE in the region of weak sites, which is usually the region where the maximum of unimodal distribution (e.g., Gaussian distribution) is located.[22] However, this model still gives meaningful results in the region of the strong adsorption sites of DASE even with columns of low efficiency.[22] The strong adsorption sites are expected to be the most interesting ones from the point of view of the interaction of the glass surface with the environment. This is the reason why in this paper we limit ourselves to the study of the strong adsorption sites region of the DASE. These strong sites adsorb molecules at a very low concentration of solute. Thus, the latter can be treated as an ideal gas. (For the same reason we simplify eq 5 with respect to the similar equation used in ref 22.)

3.2. Langmuir Equation for a Homogeneous Surface. Another model used in this paper is the Langmuir adsorption model.[23] The model describes an adsorbing surface as a collection of independent sites, each site being able to adsorb only one molecule. The probability of a site to be occupied by a molecule (or a fraction of a large group of identical sites occupied by molecules), θ, is given by the Langmuir equation

$$\theta = (1 + \exp[(\mu' - \mu)/RT])^{-1} \tag{6}$$

(This is the form of the Langmuir equation used in our previous paper.[4]) Here μ is the chemical potential of the gas (fluid) in equilibrium with the surface and μ' is the free energy of a molecule adsorbed on a site. The chemical potential of the ideal gas (as mentioned above, we consider only small concentrations) is

$$\mu = RT\ln(C/C_0) + \mu_0(T) \tag{7}$$

where $\mu_0(T)$ is the chemical potential at some standard concentration C_0 (below-standard chemical potential). To determine $\mu_0(T)$, one may use either the statistical or kinetic derivation of eq 6.[23] In the former case

$$\mu_0(T) = h_0 - Ts_0 = RT\ln(C_0 N_A \Lambda^3/Z_{int}) \qquad \Lambda = \frac{hN_A}{\sqrt{2\pi MRT}} \tag{8}$$

Here h_0 and s_0 are the standard enthalpy and entropy of the gas, respectively, h is the Plank constant, N_A is the Avogadro number, M is the molecular weight, R and T are the gas constant and temperature, respectively, and Z_{int} is the partition function

for the internal degrees of freedom of a molecule.

$$\mu' = -RT \ln Z_{ads} = U_{min} - RT \ln Z_{th} = U_{min} + \epsilon_{th} - Ts_{th} \quad (9)$$

where Z_{ads} is the partition function of an adsorbed molecule, U_{min} is the minimal energy of the molecule on a site, Z_{th} is the partition function for the energy spectrum referred to U_{min} (thermal partition function), and ϵ_{th} and s_{th} are the thermal energy and entropy, respectively.

Substitution of eq 7 in eq 6 and taking $C_0 = 1$ (in accepted units) gives another form of the Langmuir equation

$$\theta = \frac{K_H C}{1 + K_H C} \quad (10)$$

where K_H is the Henry constant. It is K_H that was determined in the majority of IGC papers on silica and glass surfaces mentioned in the Introduction. Its temperature dependence follows from eqs 8 and 9:

$$K_H = \exp(\Delta S/R) \exp(-\Delta U/RT) \quad (11)$$

$$\Delta U = U_{min} + \epsilon_{th} - h_0 \qquad \Delta S = s_{th} - s_0$$

where ΔU is the reduced energy of a site and ΔS is the reduced entropy of the site (with respect to the molecule). The temperature dependence of $\ln K_H$ vs $1/T$ is usually linear, which means that in some temperature interval ΔU and ΔS are approximately constant and can be determined from two values of K_H at different temperatures. All this is well-known and widely used in IGC study of surfaces.

However, when the Langmuir equation is used as a local isotherm $\theta(\mu,\mu',T)$ in eq 18 to describe adsorption on heterogeneous surfaces, another method of determining the energy of a site is used. In essence, it is based on an a priori evaluation of the entropy of a site. One evaluation, in fact, assigns to ΔS the value of the reduced entropy of liquid.[22,24] Another uses parameters from the kinetic derivation of the Langmuir equation to evaluate ΔS in K_H.[25,26]

The kinetic derivation of eq 6 gives[23]

$$\theta = \frac{\nu\tau C}{1 + \nu\tau C} \quad (12)$$

where νC is the number of impacts of gas molecules at concentration C on an adsorption site per unit time and

$$\nu = \sqrt{\frac{RT}{2\pi M}} \sigma \alpha N_A \quad (13)$$

Here σ is the effective area of the site, α is the sticking coefficient, and τ is the adsorption lifetime

$$\tau = \tau_0 \exp(-U_0/RT) \quad (14)$$

Designate

$$\mu = RT \ln C/C_0 + RT \ln(C_0 \nu \tau_0) + \delta\mu \quad (15)$$

$$\mu' = U_0 + \delta\mu \quad (16)$$

(if ν and τ_0 are fixed, $\delta\mu$ can, in principle, be determined from eqs 7 and 8) and substitute this equations in eq 6 to obtain eq 12. Thus, one has to evaluate α in eq 13 (the other parameters of this equation are, in fact, known) and τ_0 and assume that ΔU in eq 11 is equal to U_0 in eq 14 to find ΔS in eq 11. This, actually, has been done in ref 25 where the following estimates have been accepted: $\tau_0 = 10^{-12}$ s (the value calculated earlier for nitrogen) and $\alpha = 1$. These estimates were used in many papers (see, e.g., ref 26) even with organic molecules, which are not expected to have the values of τ_0 and α close to those for nitrogen. On the other hand, one can compare eqs 2 and 33 from ref 24 with eqs 12 and 14 to obtain

$$\frac{RT}{\nu\tau_0} = P_s \exp\left(\frac{\epsilon_v}{RT}\right) \quad (17)$$

This equation makes it possible to find $\nu\tau_0$ from eqs 12 and 14 by the method of ref 24.

Still another method of evaluation ΔS in eq 11 takes it as a constant and determines its value as that minimizing the temperature dependence of the DASE.[27] There are still other methods (see, e.g., references in refs 24 and 26) and almost all of them assume that the entropies of all adsorption sites are the same. Some exceptions from this rule are briefly discussed in pp 108, 119, and 326 of ref 17. They consider the dependence of the entropy or (equivalently) the vibration frequency of a molecule on a site upon the site energy. See also a brief discussion of this problem in the Introduction to ref 4.

As mentioned in ref 27, sometimes these methods give contradictory results. Anyway, all of them include some approximations. It will be shown in the next subsection that one can do without those approximations: One can extend the ordinary method of determination of ΔU and ΔS on a homogeneous surface mentioned above eq 11 to heterogeneous surfaces. This method gives distribution of sites in energy and entropy separately. Besides, it gives the entropy/energy relationship for sites, which makes it possible to assess the validity of these distributions. The latter is especially important because, to the best of our knowledge, at present there is no other method that can validate the distribution of sites in energy obtained from an isotherm of adsorption. The details of the new method are explained below.

3.3. Langmuir Equation for a Heterogeneous Surface. The average number of occupied sites (adsorption) on a surface consisting different sites is[4]

$$a(\mu,T) = \int_{\mu'_{min}}^{\mu'_{max}} \theta(\mu,\mu',T)\, n(\mu',T)\, d\mu' \quad (18)$$

where $n(\mu',T)$ is the distribution density of sites in free energy normalized to the number of sites per unit of surface and $\theta(\mu,\mu',T)$ is eq 6. Note that $n(\mu',T)$ depends on temperature.

To obtain $n(\mu',T)$ from $a(\mu,T)$ one has to solve the integral equation 18. One numerical method (not new) of obtaining that solution was considered in ref 4. Here we use another method that is especially convenient for a chromatography experiment. The method was developed for the Langmuir model many years ago by Temkin and Levich and was reviewed in ref 28. Later it was extended to other models[17,27] (now it is known as the Rudzinski−Jagiello method). The result is (eq 5-32 in ref 28):

$$n(x) = \frac{da}{dx} - \frac{\pi^2}{3!}\frac{d^3a}{dx^3} + \frac{\pi^4 d^5 a}{5! dx^5} - \ldots \quad (19)$$

where x on the left side designates the free energy μ' and on the right side it designates the chemical potential μ. This equation is especially convenient for application in IGC since the first term on th right-hand side is proportional to V_N in eq 5.

To obtain the distribution of sites in energy, we use the method developed in our previous paper.[4] Specifically, we use the following equations from ref 4:

$$\left(\frac{d\mu'}{dT}\right)_N = -\langle s' \rangle \tag{20}$$

and

$$\langle \epsilon' \rangle = \mu' + T\langle s' \rangle \tag{21}$$

where N is the cumulative distribution function in free energy

$$N = \int_{-\infty}^{\mu'} n(x)\, dx \tag{22}$$

In eqs 20 and 21, μ' is the free energy of a site. It is connected to the Henry constant of the site by eq 11

$$\mu' = RT \ln K_H + \mu_0 \tag{23}$$

where μ_0 is the standard chemical potential in eq 7. Thus, eqs 20 and 21 are just generalization of the widely used method of determination of the entropy and energy of adsorption from the temperature dependence of the Henry constant. The differences are that, first, $\langle s' \rangle$ and $\langle \epsilon' \rangle$ are not just the entropy and the energy of a site but averages over all the sites with the same value of the free energy μ'.[4] Second, to obtain the entropy from the Henry constant, one uses the derivative of its logarithm with respect to temperature while in eq 20 it is substituted by a partial derivative at constant N. Finally, eqs 20 and 21 are expressed in absolute values of corresponding thermodynamic functions while in experiments (eq 11 or the next section) reduced values are usually employed.

The values of s' and ϵ' in eqs 20 and 21 depend on μ' or (since $N = N(\mu')$ at constant T) on N. Thus, $\langle s' \rangle = s(N)$ and $\langle \epsilon' \rangle = \epsilon(N)$ are the (inverted) cumulative distributions of adsorption sites in entropy or energy. Excluding N from these equations, one obtains[4]

$$s' = f(\epsilon') \tag{24}$$

It was shown in ref 4 that this equation can be used to assess the reliability of a distribution of sites in energy (entropy). Its usefulness will be demonstrated below.

Finally, as mentioned above, in this section we use the absolute values of the chemical potential μ, free energy of a site μ', and the energy ϵ' and entropy s' of a site. However, eq 6 depends on the difference $\mu' - \mu$, which means that one can subtract from μ' and μ (simultaneously) any function of temperature. As a result, one obtains reduced thermodynamic functions (free energy, energy, and entropy) used in the next section.

4. Results and Discussion

Two chromatographic peaks of pure hexane are presented in Figure 1. The monolayer capacity in the column was evaluated on the grounds of the molecular area of a hexane molecule of 51.6 Å^2 [29] and the total surface area in the column of 5.9 m^2. Thus, the solid curve in Figure 1 corresponds to the loading (the ratio of injected amount to the monolayer capacity) of 16%. The internal units of the ordinate axis in Figure 1 can be transferred to concentrations by eq 2. The maximum ordinate (10^8 counts) corresponds to 0.164 mol/m^3, which, in turn, corresponds to 413.4 Pa (3.1 mmHg) of partial pressure of hexane. The saturated vapor pressure of hexane at 40° C is 280 mmHg so that the relative pressure corresponding to the maximum of the solid curve in Figure 1 is 0.009. This is definitely a submonolayer region (usually the BET monolayer on silica corresponds to relative pressure on the order of magnitude 0.1; see, e.g., Figure 2.17 in ref 29).

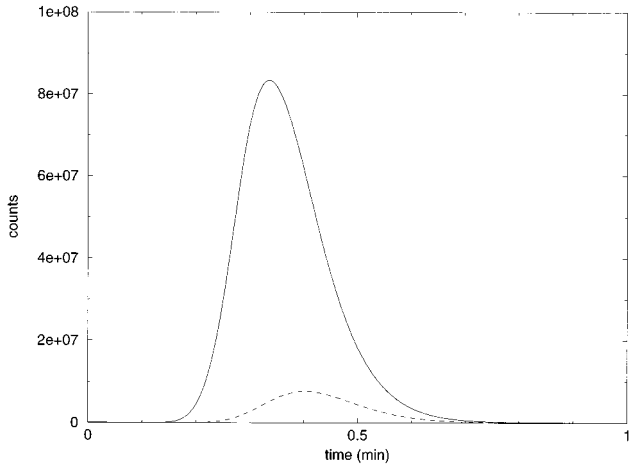

Figure 1. Experimental peaks of hexane at 40 °C. Counts are units of intensity used in HP5890. To convert them to nmol/s, multiply the ordinate by 2.42×10^{-6} (cf. section 2). Key: solid line, 3.04 μmol injected; broken line, 0.304 μmol injected. The capacity of the monolayer in the column is 19 μmol. The flow rate at the outlet is 88.4 mL/min, the pressure drop over the column is 0.3 psi, the pressure gradient correction coefficient $j = 0.99$, and the retention time of methane is 0.31 min.

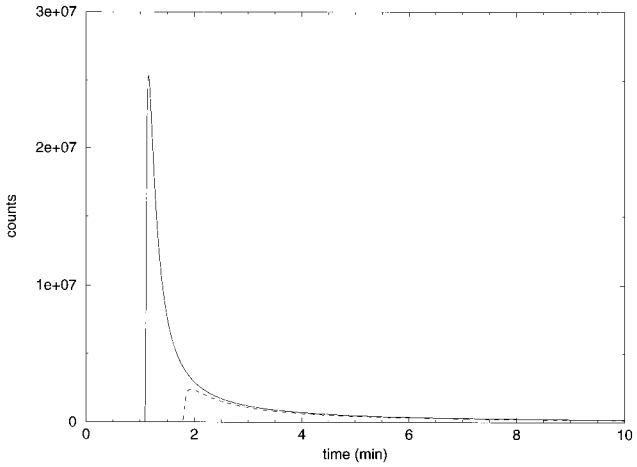

Figure 2. Experimental peaks of butanol at 100 °C: solid line, 6.548 μmol; broken line, 3.274 μmol. The flow rate is 32.3 mL/min, the pressure drop across the column is 0.6 psi, $j = 0.98$, and the retention time of methane is 0.82 ± 0.01 min.

The shapes of the peaks in Figure 1 are relatively (i.e., in comparison with those in Figure 2) symmetrical, and the positions of their maxima almost do not depend on loading. This is typical of linear equilibrium chromatography when adsorption is in the Henry region and equations of subsection 3.2 are approximately valid. However, the Ideal model described in subsection 3.1 is not valid for this case. According to this model the linear isotherm should give an infinitely narrow peak (δ-function). The broadening of the peaks in Figure 1 are due to axial diffusion in the column that is neglected in eq 3. To obtain peaks similar to those in Figure 1 from eq 3, one has to add an axial diffusion term on the right-hand side of this equation. The resulting equation is called the Semi-ideal model.[20] Finally, the solid curve in Figure 1 allows one to evaluate the effectiveness of the column. It is about 19 effective

theoretical plates. Such an unusually small effectiveness is due to small specific surfaces of the glass fiber.

Compare now the lower peak in Figure 2 (broken curve) with the higher peak in Figure 1 (solid curve). They are obtained at about the same injected amounts of solute but their shapes are drastically different. The butanol peak is much more asymmetric and much broader than that for hexane. This is despite the fact that the butanol peak is obtained at a higher temperature than that of hexane. At the temperature corresponding to Figure 1, the lower peak in Figure 2 was so broad that one could hardly observe it. The lower flow rate also makes the peaks in Figure 2 broader than those in Figure 1, but this does not change their shape. The peaks in Figure 2 were obtained on the column with a capillary at the output (see section 2). This was done to decrease the flow rate and to provide more time for establishing adsorption equilibrium in the column.

The loading of the lower peak in Figure 2 is 7% (it is less than the loading for hexane at the same injected amount because the molecular area for butanol is less). Its maximum corresponds to the concentration of butanol of 0.02 mol/m^3 and the partial pressure of 0.5 mmHg. The saturated vapor pressure of butanol at 100° C is 377 mmHg. Thus, the relative pressure of butanol at the maximum of the lower peak is 0.0013 and the isotherm is still not in the Henry region (the peak is strongly asymmetric). This can be explained only by the heterogeneity of the E-glass surface with respect to butanol. The appropriate model for this case is described in subsection 3.3.

In general, an asymmetric shape of a chromatographic peak does not necessarily mean that the surface is heterogeneous, that is, in the Langmuir model terms, is composed of different adsorption sites. In the first IGC experiments on glass fibers mentioned in the Introduction, they obtained asymmetric peaks for *n*-alkanes for which the glass surface is homogeneous, i.e., can be considered in the first approximation as composed of identical sites (see below). However, this was obtained at high loadings with a detector of lower sensitivity (katharometer).[7] When they used a much more sensitive detector of the same type as used in this paper (FID), they were able to work at much lower loadings and obtained symmetrical peaks similar to that in Figure 1 for hexane and other *n*-alkanes.[6] Thus, the peculiarity of the peaks in Figure 2 is not just that they are asymmetric but that they are asymmetric at low loadings well below the monolayer completion (see below). This is why we have to invoke the model described in subsection 3.3 to explain them.

The chromatographic experiment, part of which is shown in Figure 2, lasted for 45 min at fixed temperature. Its end is shown in Figure 3. One can see that at the end of the fixed temperature part, the relative pressure of butanol dropped 100 times with respect to its maximal value at about 1.8 min (compare ordinates of the dashed curves in Figures 2 and 3). However, many sites are still occupied by adsorbed molecules: When after 45 min the temperature raised to 250 °C (as described in section 2), the second peak appeared. The area of this peak (for the dashed curve) is 51% of the peak at 100 °C. These are molecules that were adsorbed on the strongest sites and could not be eluted by the helium flow for 45 min at 100 °C.

Thus, we have to assume that our surface is composed of different adsorption sites and use eq 19 to find distribution of these sites in free energy. First we have to calculate da/dx on the right-hand side of this equation where a is the adsorption per meter squared of the surface and x is the chemical potential of solute (butanol in helium). As mentioned in subsection 3.2, since eq 6 depends on the difference between the free energy of a site μ' and the chemical potential of the solute μ, one need not take their absolute values. We use eq 15 and designate

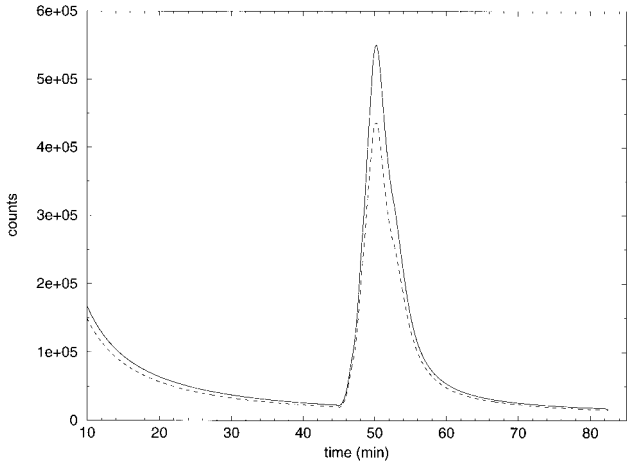

Figure 3. Continuation of Figure 2. Until 45 min parameters are the same as in Figure 2. From 45 to 49 min the temperature increases linearly up to 250 °C; after 49 min, the temperature is 250° C.

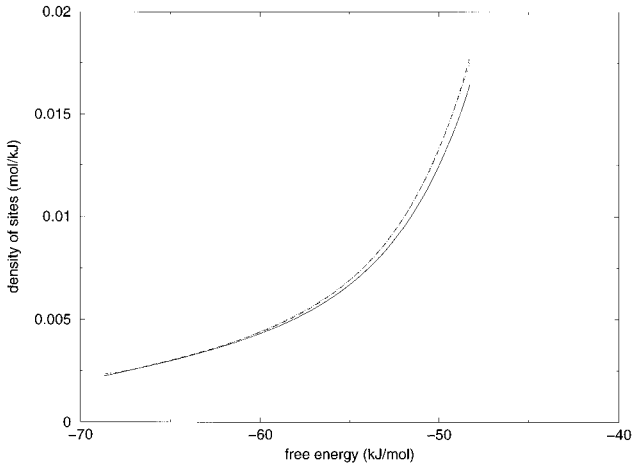

Figure 4. Distribution density of sites in free energy for the solid line in Figure 2: dotted line, first approximation; dashed line, least-squares fit; solid line, final result.

$$\Delta\mu = \mu - \delta\mu = RT \ln(C\nu\tau_0) \qquad (25)$$

with $\tau_0 = 10^{-12}$ s. In eq 13 $\sigma = 28$ Å^2[30] and $\alpha = 0.1$. The latter is an arbitrary value, and τ_0 is the Hobson's value that corresponds to nitrogen and not to butanol. However, the arbitrariness in the choice of these parameters is not important now because it is counterbalanced by the arbitrary function $\delta\mu$ in eq 25. In other words, we use a reduced value of the chemical potential, the standard potential being fixed by the above choice of τ_0 and α.

Thus, on the right-hand of eq 19, x is $\Delta\mu$ from eq 25 and $a = N/S$ where N stands on the right-hand side of eq 5 and $S = 5.9$ m^2 is the total surface in the column. Thus, da/d$x = CV_N/(SRT)$. This curve (for the solid curve in Figure 2) is presented as the dotted curve in Figure 4. (The ordinates of curves in Figure 4 are divided by the total number of sites per meter squared estimated as $1/a_m$; $a_m = 28$ Å^2.[30]) This is the first approximation for the distribution density of sites in the (reduced) free energy. To get the next approximation, one has to evaluate the second derivative of this curve. The general method of obtaining this and higher derivatives is described in ref 26. Here, we use a simpler procedure that works well for our particular case. We just obtained a least-squares polynomial

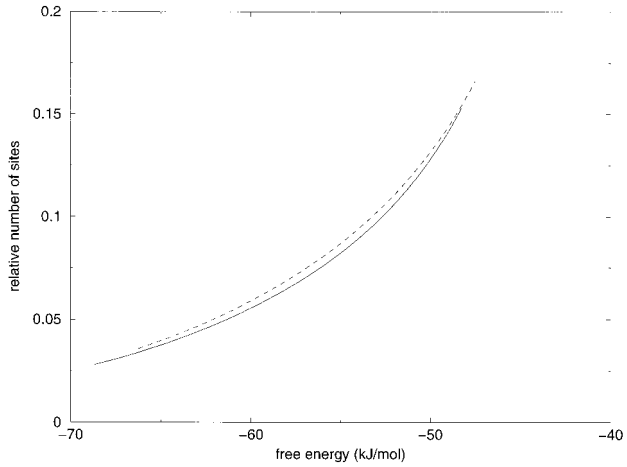

Figure 5. Distribution (cumulative) of sites in free energy: solid line, 100 °C (corresponds to the solid line in Figure 4); dashed line, 90° C.

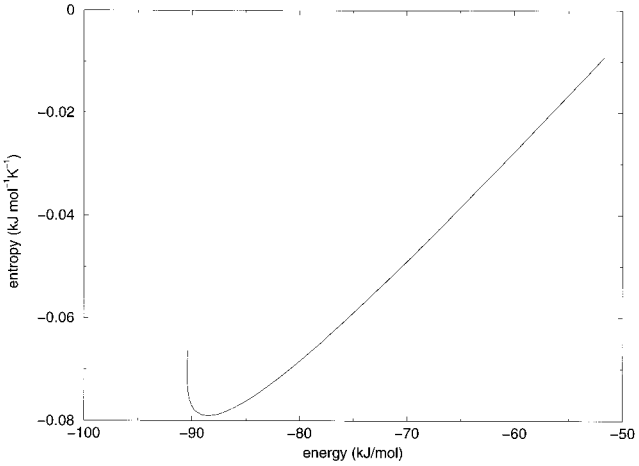

Figure 6. Entropy/energy relation for butanol.

fit of the logarithm of the dotted curve in Figure 4, which is presented as the dashed curve and calculated the second derivative of the dashed curve analytically. The distribution corresponding to the first and the second terms on the right-hand side of eq 19 is presented as the solid curve in Figure 4. It is seen that the second term on the right in eq 19 makes only a small correction to the initial evaluation of the distribution density in our particular case. Thus, we do not evaluate higher terms (and do not use the more sophisticated method of ref 26).

Then we integrate the solid curve in Figure 4 to obtain the distribution function (cumulative) in free energy. As an initial value (constant of integration) we take the number of sites corresponding to the peak (solid line) in Figure 3. These are all the sites whose retention time is larger than 45 min and free energy is smaller than −68 kJ/mol. The distribution functions in free energy are presented in Figure 5 for two temperatures. Now we use eqs 20 and 21 to obtain distribution functions (cumulative) for entropy and the energy separately and, most importantly, the entropy/energy relation presented in Figure 6. Since the abscissa in Figure 5 is not the absolute but reduced free energy, so is the entropy in Figure 6 (which is why it is negative). The value of energy is also reduced, which means that it is not strictly equal to ΔU in eq 11. However, the relative difference between ΔU and reduced energy in Figures 6 and 7 is not as big as that for entropy because the energy (absolute or reduced) is dominated by U_{min}.

The linear relation between entropy and energy (enthalpy) is known in many branches of physical chemistry (see references

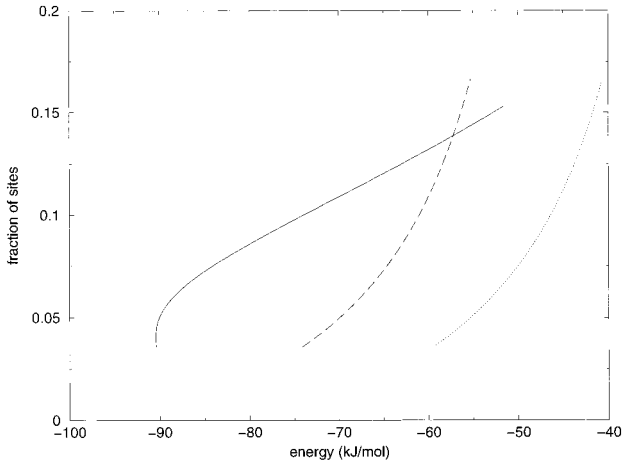

Figure 7. Distribution (cumulative) of adsorption sites in energy of butanol. The fraction of sites means the number of sites with energy less than the abscissa of the point divided by the maximal number of sites. The maximal number of sites (per meter squared) is $1/a_m$ (a_m = 28 Å^2). The solid curve corresponds to distributions of Figure 5 and is obtained by eq 21. The dashed and dotted curves are obtained on assumption of constant entropy of sites: dashed curve, method from ref 24, eq 17; dotted curve, method.[25]

in ref 31). In the present context it means that the stronger the adsorption site, the less is the thermal entropy of a molecule absorbed on that site, i.e., the stronger is the constriction imposed by the site on the molecule. The inverse slope of this linear relation is sometimes called the isokinetic temperature T_i. For the linear part of the plot in Figure 6, $T_i = 467$ K. This is lower than $T_i = 800$ K that was experimentally observed for argon and nitrogen on active coal and other absorbents or $T_i = 740$ K obtained by computer simulation for argon on a model oxide surface.[31] The smaller is T_i, the stronger is the decrease of entropy of a molecule with an increase of site strength. One would expect that for a relatively long and flexible butanol molecule the decrease of entropy with an increase of the strength of adsorption site should be larger than for a small and rigid molecule like argon or nitrogen. Therefore, the fact that the isokinetic temperature for butanol observed here is smaller (although of comparable magnitude) than those for argon or nitrogen seems reasonable.

However, at the left end of the plot in Figure 6 its slope becomes negative. This behavior of the plot in Figure 6 corresponds to a steep drop at the strong sites side of the distribution curve in Figure 7. The latter could have been interpreted as a fact that the strongest site on our surface has the energy of about −90 kJ/mol. However, the unrealistic behavior of the entropy/energy plot in this area shows that this is not the case and the corresponding part of the distribution in Figure 7 is an artifact—the result of experimental errors.

The source of these errors is probably the Ideal model, which is the foundation of our calculation. As described in subsection 3.1, this model is accurate only for columns of high efficiency. For low efficient columns it is totally inapplicable in the monolayer region (weak adsorption sites portion of the distribution). But in the region of strong adsorption sites this model is also not very accurate for low efficient columns. One may see in Figure 3 that the solid curve (higher loading) goes above the dashed curve. This is in contradiction with the Ideal model according to which they should coincide. This inaccuracy of the Ideal model is not as large as it is in the monolayer region[22] but it still might be the source of error in the strong adsorption sites portion of the distribution.

The distributions in Figure 7 are cumulative distributions, which means that the ordinate of a point on a curve is a fraction of sites whose energies are lower than the abscissa of the point. To obtain such a plot, one needs not only the chromatographic peak like those in Figure 2 but also the number of residual molecules on the surface given by the areas of the peaks in Figure 3. If converted to the distribution density (differentiated with respect to energy), it will look rather unusual: It is only the strong site tail of a plot that usually has one or more maxima (cf., e.g., distribution densities in refs 11, 13, 26, and 27). There are three reasons why we limit ourselves by this portion of the energy distribution. First, as mentioned above, the Ideal model cannot give the weak site portion of the distribution with columns of low efficiency. Second, the Langmuir model, which assumes that each site can be occupied by only one molecule and there is no correlation in occupations of different sites, is much more applicable to strong sites than to weak ones. (In part, this is because the strong sites adsorb at lower loadings when average distances between adsorbed molecules are relatively large and the interaction between those molecules is much less than interactions of those molecules with sites.) Third, we believe that the strong sites portion of the *cumulative* energy distribution of sites is the most important one because these sites determine the interaction of a glass surface with the environment.

The strong sites in Figure 7 are also the most interesting ones from the point of view of our previous work, where we used adsorbed molecules as probes for the atomic structure of an amorphous silica surface.[1,2] It was shown that the sites that interact most strongly with water molecules are those where the intensity of the electrostatic field is the strongest.[1] The same should be true for other polar molecules, in particular for butanol, and not only for amorphous silica but for other silicate glasses as well. We have also shown that the surface of amorphous silica is almost (all surfaces are more or less heterogeneous) homogeneous for argon.[2] This is because the irregular electrostatic field almost does not interact with nonpolar argon molecules. This result agrees nicely with what we observe in this work for nonpolar hexane and polar butanol. The dramatic qualitative difference between the peak profiles in Figures 1 and 2 is explained by the fact that the surface of our glass is almost homogeneous for hexane and strongly heterogeneous for butanol. One may also notice that the profile of the hexane peak in Figure 1 has some small asymmetry (it is also broader than the methane peak) that may be an indication of the small heterogeneity of the surface. However, as mentioned above, this heterogeneity cannot be quantitatively assessed on the grounds of the Ideal model.

The dotted curve in Figure 7 is the distribution function calculated by the method of 25 (see subsection 3.2). The method was developed for nitrogen and it is not astonishing that it gives inappropriate results for butanol. A better result (dashed curve in Figure 7) is obtained by the method of 24 (eq 17 in our terms). However, both dashed and dotted curves deviate considerably from the solid curve in Figure 7. This is because both of them assume that the entropies of sites are constant while Figure 6 clearly shows that this is not the case for butanol. The fact that the variation of the site entropies can be neglected in calculations of the energy distribution functions was substantiated theoretically for simple molecules (see references in ref 24). Although it was known long ago (see at the end of subsection 3.2) that the vibration frequencies of a molecule on a site (and therefore the entropy of the site) depend on the site energy, this fact could be neglected because for simple and rigid molecules (like nitrogen or rare gases for which the majority of the energy distribution were published) the whole entropy term in the free energy is much smaller than the energy term. Our result shows that this assumption is not valid any more for larger and flexible molecules such as butanol.

From Figure 3 and eq 2, one may calculate that the concentration of butanol at the output of the column at 45 min at the temperature of the column 100 °C was 0.2 mmol/m^3 (corresponding to a partial pressure of 0.005 mmHg). This corresponds to the retention time of the strongest site in Figure 7. Take, for example, the site with the energy of −85 kJ/mol. Its reduced entropy is −0.076 kJ mol^{-1} K^{-1} (Figure 6). Thus, the free energy of the site $\Delta\mu' = -56.7$ kJ/mol. According to eq 6, half of these sites will be empty when $\Delta\mu = \Delta\mu'$, where $\Delta\mu$ is determined by eq 25. According to eq 13 with the values of α and τ_0 mentioned above, $\nu\tau_0 = 1.36 \times 10^{-6}$ m^3/mol for butanol and $C = 8$ mmol/m^3. Suppose now that a site is 2 times stronger with the free energy of −113.4 kJ/mol. Similar calculation shows that half of these sites will be empty at a concentration of butanol equal to 0.1 nmol/m^3. The sensitivity of our chromatograph is determined by the background, which is about 10 counts. At the flow rate of 30 mL/min, according to eq 2, the minimal concentration of butanol that can be detected is 80 nmol/m^3, which is 800 times higher than the concentration of butanol necessary to make half of the sites with free energy −113.4 kJ/mol empty at 100 °C. The isotherm of adsorption on a heterogeneous surface is in the Henry region when the strongest sites are in this region, i.e., when more than half of the strongest sites are empty. This example shows why, contrary to the widespread belief (cf., e.g., ref 10), one may be unable to experimentally reach the Henry region on a glass surface. Experiments with nitrogen and rare gases at their boiling temperatures mentioned in the Introduction confirm that this really might be the case.

5. Conclusion

The surface of E-glass studied in this paper is homogeneous with respect to adsorption of hexane and heterogeneous with respect to adsorption of butanol. This result was obtained experimentally by the method of inverse gas chromatography and concurs nicely with our previous finding by computer simulation that the surface of amorphous silica is homogeneous with respect to adsorption of argon and heterogeneous with respect to adsorption of water or carbon dioxide (see Introduction).

We applied here a new method of adsorption data analysis that was put forth in our previous paper.[4] This method allows one to obtain distribution functions of adsorption sites in energy and in entropy separately and without any preliminary assumptions. It is shown here that it is an extension of the well-known method of obtaining enthalpy and entropy from two Henry constants at different temperatures. It is also shown that the distribution of adsorption sites in energy obtained for butanol with the help of the new method deviates considerably from those obtained by previous methods. The reason for the deviation is the assumption that the entropy of all sites are the same that was made in those methods. This assumption might be reasonable for a light and rigid molecule like nitrogen but is inapplicable to a relatively large and flexible molecule like butanol.

In addition to that, the method allows one to obtain the entropy/energy relation for different adsorption sites. This curve helps to detect unreliable portions of the energy distribution of sites.

We believe that although these results are qualitatively true (and the new method mentioned above is certainly true) additional work is necessary to make IGC a reliable method for adsorption study of glass fibers. First of all, it is necessary to develop a method of obtaining isotherms of adsorption from chromatographic peak profiles obtained with columns of low efficiency because the Ideal model of chromatography is only of limited use in this case.

Acknowledgment. This material is based upon work supported by the National Science Foundation under grant no. DMR 9803884. We are thankful to Restek Corp. for help in preparing chromatographic columns and to W. A. Steele for discussion of the paper.

References and Notes

(1) Bakaev, V. A.; Steele, W. A. *J. Chem. Phys.* **1999**, *111*, 9803.

(2) Bakaev, V. A.; Steele, W. A.; Bakaeva, T. I.; Pantano, C. G. *J. Chem. Phys.* **1999**, *111*, 9813.

(3) Bakaev, V. A. *Phys. Rev. B* **1999**, *60*, 10723.

(4) Bakaeva, T. I.; Pantano, C. G.; Bakaev, V. A. *Langmuir* **2000**, *16*, 5712.

(5) Saint Flour, C.; Papirer, E. *Ind. Eng. Chem. Prod. Res. Dev.* **1982**, *21*, 337.

(6) Saint Flour, C.; Papirer, E. *Ind. Eng. Chem. Prod. Res. Dev.* **1982**, *21*, 666.

(7) Saint Flour, C.; Papirer, E. *J. Colloid Interface Sci.* **1983**, *91*, 69.

(8) Osmont, E.; Schreiber, H. P. In *Inverse Gas Chromatography. Characterization of Polymers and Other Materials*; Lloyd, D. R., Ward, T. C., Schreiber, H. P., Pizaña, C. C., Eds.; American Chemical Society: Washington, DC, 1989.

(9) Anthony, L. J.; Holland, R. A. *J. Non-Cryst. Solids* **1990**, *120*, 82.

(10) Tiburcio, A. C.; Manson, J. A. *J. Appl. Polym. Sci.* **1991**, *42*, 427.

(11) Jaroniec, M. In *Adsorption on New and Modified Inorganic Sorbents*; Dabrowski, A., Tertykh, V. A., Eds.; Elsevier: Amsterdam, 1996.

(12) Voelkel, A. In *Adsorption on New and Modified Inorganic Sorbents*; Dabrowski, A., Tertykh, V. A., Eds.; Elsevier: Amsterdam, 1996.

(13) Papirer, E.; Balard, H. In *Adsorption on New and Modified Inorganic Sorbents*; Dabrowski, A., Tertykh, V. A., Eds.; Elsevier: Amsterdam, 1996.

(14) Rayss, J. In *Adsorption on New and Modified Inorganic Sorbents*; Dabrowski, A., Tertykh, V. A., Eds.; Elsevier: Amsterdam, 1996.

(15) Garzón, F. J. L.; Garcia, M. D. In *Adsorption on New and Modified Inorganic Sorbents*; Dabrowski, A., Tertykh, V. A., Eds.; Elsevier: Amsterdam, 1996.

(16) Tarasevich, Yu. I.; Aksenenko, E. V.; Bondarenko, S. V. In *Adsorption on New and Modified Inorganic Sorbents*; Dabrowski, A., Tertykh, V. A., Eds.; Elsevier: Amsterdam, 1996.

(17) Rudzinski, W.; Everett, D. H. *Adsorption of Gases on Heterogeneous Surfaces*; Academic Press: London, 1992.

(18) Hobson, J. P. *Canad. J. Phys.* **1965**, *43*, 1941.

(19) Katsanos, N. A.; Thede, R.; Roubani-Kalantzopoulou, F. *J. Chromatogr. A* **1998**, *795*, 133.

(20) Katti, A. M.; Guiochon, G. A. In *Advances in Chromatography*; Giddings, J. C., Grushka, E., Brown, P. R., Eds.; Marcel Dekker: New York, 1992; Vol. 31.

(21) Conder, J. R.; Young, C. L. *Physicochemical Measurement by Gas Chromatography*; J. Wiley & Sons: Chichester, U.K., 1979.

(22) Stanley, B. J.; Guiochon, G. *Langmuir* **1994**, *10*, 4278.

(23) Bruch, L. W.; Cole, M. W.; Zaremba, E. *Physical Adsorption: Forces and Phenomena*; Clarendon Press: Oxford, U.K., 1997.

(24) Jaroniec, M. *Surf. Sci.* **1975**, *50*, 553.

(25) Hobson, J. P. *Can.. J. Phys.* **1965**, *43*, 1934.

(26) Balard, H. *Langmuir* **1997**, *13*, 1260.

(27) Jagiello, J.; Linger, G.; Papirer, E. *J. Colloid Interface Sci.* **1990**, *137*, 128.

(28) Honig, J. M. *Ann. N. Y. Acad. Sci.* **1958**, *58*, 741.

(29) Gregg, S. J.; Sing, K. S. W. *Adsorption, Surface Area and Porosity*, 2nd ed.; Academic Press: London, New York,., 1982.

(30) McClellan, A. L.; Harnsberger, H. F. *J. Colloid Interface Sci.* **1967**, *23*, 577.

(31) Bakaev, V. A. *Surf. Sci.* **1988**, *198*, 571.